Thermodynamics and Kinetics of Folding of Common-Type Acylphosphatase: Comparison to the Highly Homologous Muscle Isoenzyme[†]

Niccolò Taddei,[‡] Fabrizio Chiti,[§,||] Paolo Paoli,[‡] Tania Fiaschi,[‡] Monica Bucciantini,[‡] Massimo Stefani,[‡] Christopher M. Dobson,[§] and Giampietro Ramponi*,[‡]

Department of Biochemical Sciences, University of Florence, Viale Morgagni, 50, 50134 Florence, Italy, and Oxford Centre for Molecular Sciences, New Chemistry Laboratory, University of Oxford, South Parks Road, Oxford OX1 3QT, U.K.

Received September 21, 1998; Revised Manuscript Received December 1, 1998

ABSTRACT: The thermodynamics and kinetics of folding of common-type acylphosphatase have been studied under a variety of experimental conditions and compared with those of the homologous muscle acylphosphatase. Intrinsic fluorescence and circular dichroism have been used as spectroscopic probes to follow the folding and unfolding reactions. Both proteins appear to fold via a two-state mechanism. Under all the conditions studied, common-type acylphosphatase possesses a lower conformational stability than the muscle form. Nevertheless, common-type acylphosphatase folds more rapidly, suggesting that the conformational stability and the folding rate are not correlated in contrast to recent observations for a number of other proteins. The unfolding rate of common-type acylphosphatase is much higher than that of the muscle enzyme, indicating that the differences in conformational stability between the two proteins are primarily determined by differences in the rate of unfolding. The equilibrium *m* value is markedly different for the two proteins in the pH range of maximum conformational stability (5.0−7.5); above pH 8.0, the *m* value for common-type acylphosphatase decreases abruptly and becomes similar to that of the muscle enzyme. Moreover, at pH 9.2, the dependencies of the folding and unfolding rate constants of common-type acylphosphatase on denaturant concentration (m_f and m_u values, respectively) are notably reduced with respect to pH 5.5. The pH-induced decrease of the *m* value can be attributed to the deprotonation of three histidine residues that are present only in the common-type isoenzyme. This would decrease the positive net charge of the protein, leading to a greater compactness of the denatured state. The folding and unfolding rates of common-type acylphosphatase are not, however, significantly different at pH 5.5 and 9.2, indicating that this change in compactness of the denatured and transition states does not have a notable influence on the rate of protein folding.

Our understanding of how a protein folds into its native conformation has improved substantially in the past few years as a result of the development of new experimental techniques and theoretical methods. Such methodological improvements have enabled us to follow in detail the structural changes that occur during the folding process of a number of proteins (*1*−*3*). Different models of protein folding have been proposed, some of them based on simple two-state kinetics and others implying the existence of folding intermediates (*4*−*7*). As a general rule, proteins containing more than 100 residues fold through a multiphasic process involving the formation of stable intermediates, whereas smaller proteins and structured polypeptides follow a two-state mechanism often associated with fast and efficient folding (*6*, *8*). A more recent view, based on theoretical models and molecular simulations, suggests that the fundamental mechanism of protein folding is the same for different proteins and that differences in the folding behavior can be explained primarily as a result of differences in the balance between entropic and enthalpic contributions to the free energy of the system (*9*). Factors determining folding rates for given proteins are not, however, well understood, and a comparison of the folding properties of structurally similar proteins is one of the possible ways to address this issue.

Acylphosphatases (AcPs)[1] are small cytosolic enzymes, typically composed of 98 amino acid residues, catalyzing the hydrolysis of acyl phosphates of physiological relevance such as 1,3-bisphosphoglycerate, carbamoyl phosphate, and β-aspartyl phosphate (*10*). The biological role of AcP has

[†] This work is a contribution of the Oxford Centre for Molecular Sciences which is supported by BBSRC, EPSRC, and MRC. F.C. is supported by a grant from the EC (contract B104-CT96-5113). The research of C.M.D. is supported, in part, by an International Research Scholars award from the Howard Hughes Medical Institute and by the Wellcome Trust. The work has also been supported by funds from Italian CNR (Progetto Finalizzato "Biotecnologie"), from MURST (Progetto "Biologia Strutturale"), and from the Cassa di Risparmio di Firenze.

* Address correspondence to this author at the Department of Biochemical Sciences, Viale Morgagni, 50, 50134 Florence, Italy. Telephone: +39 55 413765. Fax: +39 55 4222725. E-mail: ramponi@scibio.unifi.it.

[‡] University of Florence.

[§] University of Oxford.

[||] On leave from the Department of Biochemical Sciences, University of Florence.

[1] Abbreviations: CT AcP, common-type acylphosphatase; M AcP, muscle acylphosphatase; Cys21Ser, cysteine 21 to serine mutated acylphosphatase; SDS−PAGE, sodium dodecyl sulfate−polyacrylamide gel electrophoresis; CD, circular dichroism; PPI, peptidyl prolyl isomerase.

10.1021/bi9822630 CCC: $18.00
Published on Web 01/26/1999

not been completely determined, although there are suggestions about its involvement in the regulation of membrane cation transport through the hydrolysis of phosphorylated amino acid residues formed during the action of the membrane ATPases (*11*, *12*). The protein has been found in all vertebrates as two highly homologous isoenzymes, named muscle- and common-type acylphosphatase (M and CT AcP, respectively; *10*). The human isoforms share 55% sequence identity. ^{1}H NMR and X-ray crystallography have shown that the proteins have very similar three-dimensional structures consisting of an antiparallel five-stranded β-sheet packed against two antiparallel α-helices with a 4-1-3-2 strand topology (*13*, *14*).

In this paper, we report a complete thermodynamic and kinetic study of folding of CT AcP by means of fluorescence and circular dichroism spectroscopies. The results are discussed in light of the data obtained recently for M AcP (*15*, *16*).

MATERIALS AND METHODS

Materials. Human CT and M AcP were expressed and purified as reported previously (*17*). The purity of the protein samples was checked by SDS–PAGE analysis (*18*). All chemicals used were analytical grade or the best commercially available.

Heat- and Urea-Induced Denaturation Experiments. Experiments were carried out on a Jasco J720 spectropolarimeter equipped with a thermostated cell holder and a NesLab model RTE-111 refrigerated water circulator. The far-UV signal at 222 nm was used to monitor thermal and urea unfolding of samples in 50 mM acetate buffer (pH 5.5) at a protein concentration of 0.4 mg/mL. Thermal and urea unfolding curves were recorded as described previously (*15*). Reversibility of unfolding was determined by measuring the CD signal at room temperature after cooling a thermally denatured sample or diluting a urea-denatured sample. The apparent equilibrium constants for unfolding calculated in the transition region were subjected to van't Hoff analysis as reported previously (*15*). Plots of ellipticity and fluorescence as a function of urea concentration were analyzed as described previously (*19*).

Conformational Stability at Different pH Values and Ionic Strengths. Urea-induced denaturation experiments were also carried out at different pH values, ranging from 2.0 to 11.5, and, at pH 5.5, in the presence of increasing sodium acetate concentrations. Tryptophan intrinsic fluorescence was used as a probe to monitor CT AcP unfolding at 25 °C, using a Shimadzu model RF-5000 spectrofluorophotometer with excitation and emission wavelengths of 280 and 335 nm, respectively, and a 10 mm path length quartz cuvette at a protein concentration of 0.02 mg/mL. In the analysis at different pH values, the following buffer solutions were used: 50 mM citric acid, pH 2.0–3.5; 50 mM formic acid, pH 3.5–4.0; 50 mM acetic acid, pH 4.0–5.5; 50 mM cacodylic acid, pH 5.5–7.0; 50 mM tris/acetic acid, pH 7.0–9.2; and 50 mM triethylamine/acetic acid, pH 9.5–11.5. The actual ionic strength of each sample containing different sodium acetate concentrations was calculated from the Henderson–Hasselbach equation and corrected by the activity coefficient. Fresh urea stock solutions were prepared and used as described previously (*15*). Plots of fluorescence signal as a function of urea concentration were treated as previously described (*19*).

Kinetic Analysis. The unfolding and refolding reactions were followed on an Applied Photophysics model SX.17MV stopped-flow fluorimeter at an excitation wavelength of 280 nm by monitoring the total fluorescence emission change. All the experiments were performed at 28 °C in 50 mM acetate buffer (pH 5.5) or 50 mM tris/acetic acid (pH 9.2), and at a final protein concentration of 0.08 mg/mL as reported previously (*16*). The fluorescence traces were fitted to single- or double-exponential functions by using the software provided by Applied Photophysics. The folding rate constants at low urea concentrations were corrected as described previously (*20*). The natural logarithms of the estimated folding and unfolding rate constants were plotted versus the urea concentration and the data fitted to the following equation (*21*):

$$\ln(k_{\mathrm{obs}}) = \ln[k_{\mathrm{f,H_2O}} \exp(-m_{\mathrm{f}}[\mathrm{urea}]) + k_{\mathrm{u,H_2O}} \exp(m_{\mathrm{u}}[\mathrm{urea}])] \quad (1)$$

where $k_{\mathrm{f,H_2O}}$ and $k_{\mathrm{u,H_2O}}$ are the folding and unfolding rate constants in the absence of urea and m_{f} and m_{u} are the slopes of ln k versus urea concentration for folding and unfolding, respectively. Such kinetic parameters were subsequently used for calculating m, $\Delta G(\mathrm{H_2O})$, and C_{m} as described previously (*21*). The urea $\alpha^{\ddagger}$ value was defined as $m_{\mathrm{u}}/(m_{\mathrm{u}} + m_{\mathrm{f}})$. The folding rate of CT AcP was also studied at various temperatures ranging from 5 to 45 °C, in 50 mM acetate buffer (pH 5.5). The data were subjected to Eyring analysis according to the methods of Chen et al. (*22*), and the changes of heat capacity ($\Delta C_{pf}^{\ddagger}$), entropy ($\Delta S_{\mathrm{f}}^{\ddagger}$), enthalpy ($\Delta H_{\mathrm{f}}^{\ddagger}$), and free energy ($\Delta G_{\mathrm{f}}^{\ddagger}$) upon moving from the unfolded to the transition state for folding at a reference temperature T_0 could be determined.

Experimental Error Determination. Curve fitting has been performed by using the software package Kaleidagraph (Abelbeck Software). Best-fit parameters and their confidence intervals expressed as one standard deviation are given for each fit. The experimental errors of the parameters calculated from measured values are standard deviations propagated according to the laws of statistics.

RESULTS

Temperature Dependence of the Conformational Stability of CT AcP. Heat and urea denaturation curves of CT AcP monitored by far-UV CD show typical two-state unfolding behavior with well-defined pre- and post-transition baselines and a single sharp transition (Figure 1A,B). Urea-induced unfolding, studied using intrinsic fluorescence as a probe, also features a single transition. The fluorescence-detected transition overlays that monitored by far-UV CD, suggesting a single-step unfolding process, characterized by the cooperative loss of native structure (Figure 1B). Both thermal and chemical denaturation were found to be fully reversible under these conditions.

Urea denaturation curves were acquired at temperatures ranging from 5 to 40 °C at approximately 5 °C intervals. The raw data were analyzed as described in Materials and Methods, and the parameters determined by such analysis are given in Table 1. The m value was found to be

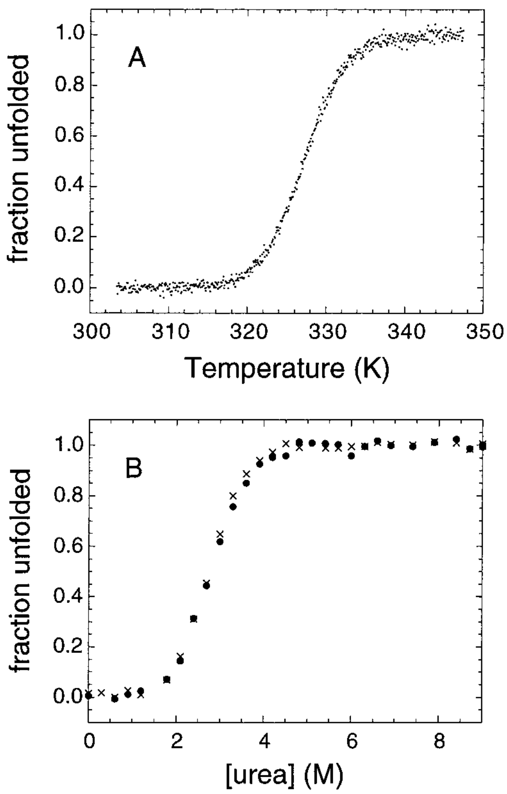

FIGURE 1: Heat- (A) and urea-induced (B) denaturation of CT AcP in 50 mM acetate buffer (pH 5.5). Thermal denaturation was followed by far-UV CD at 222 nm and urea denaturation by far-UV CD at 222 nm (circles) and intrinsic tryptophan fluorescence (crosses) at 28 °C. The raw data have been converted to the fraction of unfolded protein by using $f_u = (y - y_n)/(y_d - y_n)$, where y_n and y_d are the signals of the native and denatured protein, respectively, and extrapolated to the temperature or urea concentration under consideration.

Table 1: Analysis of Urea-Induced Denaturation Curves of CT AcP at pH 5.5[a]

temperature (°C)	C_m (M)	m (kJ mol^{-1} M^{-1})	$\Delta G(H_2O)$ (kJ mol^{-1})
5	3.19	7.3	20.2
10	3.18	6.5	20.1
15	3.16	6.2	20.0
20	3.05	5.6	19.3
25	2.89	6.2	18.3
30	2.45	5.4	15.5
35	2.05	6.6	13.0
40	1.52	6.7	9.6

[a] Data were processed as described in Materials and Methods. The m value is, to a good approximation, temperature-independent, and an averaged m value of 6.32 ± 0.49 kJ mol^{-1} M^{-1} was calculated. The $\Delta G(H_2O)$ values were obtained by using the averaged m value. Experimental errors are ca. 0.10 M for C_m, 0.6 kJ mol^{-1} M^{-1} for m, and 8% for $\Delta G(H_2O)$.

approximately independent of temperature, and an average value of 6.32 ± 0.49 kJ mol^{-1} M^{-1} was used for recalculating $\Delta G(H_2O)$ values. Unlike the m value, the midpoint of urea denaturation (C_m) undergoes a significant decrease upon increasing the temperature, thereby causing a corresponding decrease in the $\Delta G(H_2O)$ value. Following the procedure of Agashe and Udgaonkar (*23*), a plot of $\Delta G(H_2O)$ versus temperature was constructed by combining the values of $\Delta G(H_2O)$ obtained by urea denaturation at various temperatures with the ΔG values obtained within the transition of a single heat denaturation experiment in the absence of

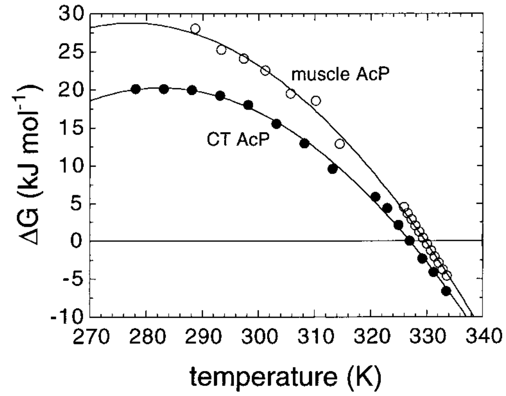

FIGURE 2: Free energy of unfolding of CT AcP (●) at pH 5.5 as a function of temperature (stability curve). The data at high temperatures (320−334 K) were obtained from a single heat denaturation experiment in the absence of urea, whereas each ΔG value at lower temperatures (275−315 K) has been extrapolated from a single urea-induced unfolding experiment performed at the indicated temperature. The solid line through the data results from the best fit to eq 2, with the parameters reported in Table 2. The data corresponding to M AcP (○) are also reported for comparison and were obtained by Chiti et al. (*15*).

Table 2: Thermodynamic Parameters of AcP from the Analysis of the Stability Curve[a]

protein	T_m (K)	ΔH_m (kJ mol^{-1})	ΔS_m (kJ mol^{-1} K^{-1})	ΔC_p (kJ mol^{-1} K^{-1})	T_s (K)	ΔG_s (kJ mol^{-1})
CT AcP	327.0	290	0.89	6.10	283	20.2
M AcP	329.7	350	1.06	6.35	277	28.7

[a] For CT AcP, values of T_m, ΔH_m, and ΔC_p were derived by fitting the data of the stability curve (Figure 2) to eq 2. ΔS_m was subsequently calculated using $\Delta S_m = \Delta H_m/T_m$. T_s and ΔG_s are the temperature and free energy of maximum conformational stability and were calculated according to the methods of Chiti et al. (*15*). The parameters of M AcP are those reported by Chiti et al. (*15*). Experimental errors from the least-squares fits are as follows: 10% for ΔC_p, 5% for ΔH_m, 10% for ΔS_m, 0.5 and 2 K for T_m and T_s, respectively, and 10% for ΔG_s.

denaturant (Figure 2). The data were fitted to

$$\Delta G(T) = \Delta H_m(1 - T/T_m) + \Delta C_p[T - T_m - T\ln(T/T_m)] \quad (2)$$

where T_m is the temperature at which the protein is half-denatured, ΔH_m is the enthalpy change upon unfolding at T_m, and ΔC_p is the heat capacity change due to unfolding (*23*, *24*). The parameters obtained by the fitting procedure, together with the corresponding values relative to M AcP, are reported in Table 2. The estimate of the ΔC_p value is important for studying the temperature dependence of ΔG, ΔH, and ΔS of AcP folding. At 25 °C, ΔH and $T\Delta S$ were calculated to be 114 ± 15 kJ mol^{-1} and 96 ± 12 kJ mol^{-1} K^{-1}, respectively. Figure 2 shows that the conformational free energy of CT AcP is significantly lower than that of M AcP over the entire range of temperatures under consideration. Similarly, the resistance of CT AcP to thermal and chemical denaturation is reduced significantly compared to that of M AcP at pH 5.5 as judged by T_m (53.9 ± 0.5 vs 56.6 ± 0.5 °C) and C_m (2.89 ± 0.10 vs 4.50 ± 0.10 M, at 25 °C) values.

Urea-Induced Denaturation upon Variation of pH and Ionic Strength. The stability of CT AcP was also studied over a wide range of pH values by means of urea denaturation experiments. Figure 3 depicts estimates of C_m, m, and

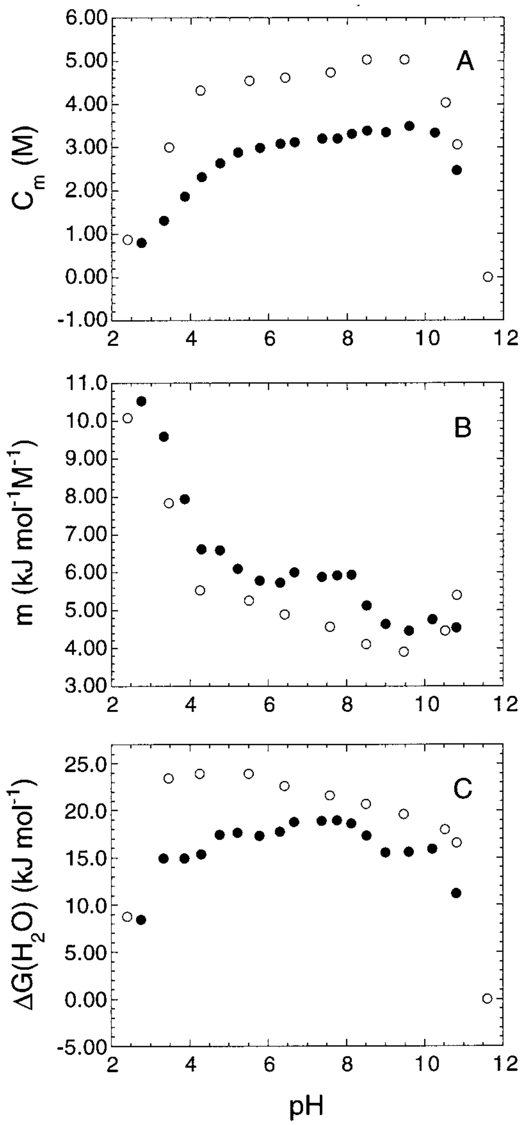

FIGURE 3: pH dependence of C_m (A), *m* value (B), and $\Delta G(H_2O)$ (C) of urea-induced unfolding of CT AcP (black symbols) and M AcP (white symbols). The latter data are those reported by Chiti et al. (*15*). Experimental errors for C_m are indicated by the size of the symbols; for *m* and $\Delta G(H_2O)$, values are approximately 7%.

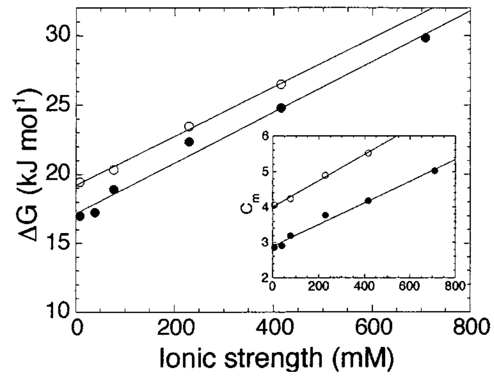

FIGURE 4: Dependence of $\Delta G(H_2O)$ on ionic strength as calculated from urea denaturation experiments at different acetate concentrations at pH 5.5 and 25 °C for CT AcP (black symbols) and M AcP (white symbols). In the inset is depicted the dependence of C_m values on ionic strength under the same experimental conditions. Experimental errors for $\Delta G(H_2O)$ and C_m values are ca. 5% and 0.10 M, respectively.

$\Delta G(H_2O)$ in the range of pH 2.7−11.0, together with the corresponding values found for M AcP under the same conditions (*15*). As can be seen, the pH dependencies of C_m and *m* are in the opposite direction. The midpoint of denaturation was found to collapse abruptly at very low and very high pH values, as expected in the presence of an excess of positive (or negative) charges at extremes of pH (*25*). The maximum resistance of CT AcP against urea denaturation was found to be close to pH 9.0 ($C_m = 3.41 \pm 0.10$ M) with little variation in the pH range of 5.0−8.5 and an averaged C_m value of 3.22 ± 0.10 M. By contrast, the lowest values of *m* are in the pH range of 8.5−11.0 (average $m = 4.60 \pm 0.13$ kJ mol^{-1} M^{-1}), and a sharp increase is observed at about pH 8.0 to an average value of 5.91 ± 0.13 kJ mol^{-1} M^{-1} in the pH range of 5.0−7.5. Finally, a dramatic enhancement of the *m* value was found at acidic pH values with a maximum value of 10.5 ± 0.8 kJ mol^{-1} M^{-1} below pH 3.0. Interestingly, the abrupt decrease of the *m* value above pH 8.0 was not observed for M AcP. Such a reduction in the *m* value without an accompanying change in C_m value is responsible for the reduced conformational stability of CT AcP in the high pH range [average $\Delta G(H_2O) = 15.7 \pm 1.1$ kJ mol^{-1}]. The highest conformational stability has been found at about pH 7.5 [$\Delta G(H_2O) = 18.8 \pm 1.3$ kJ mol^{-1}].

The stability of CT AcP was also studied as a function of ionic strength through urea-induced denaturation experiments, and has been compared to similar data obtained for M AcP. The salt used to vary the ionic strength of the samples was sodium acetate rather than the commonly used sodium chloride, due to the potential of the chloride ion to affect the AcP stability through specific binding to the active site of the enzyme (*26*). The *m* value appears to be independent of the salt concentration for both isoenzymes (average values of 5.95 ± 0.54 and 4.80 ± 0.45 kJ mol^{-1} M^{-1} for CT and M AcP, respectively). Figure 4 indicates that the C_m and the conformational stability of both proteins increase linearly with increasing ionic strength over the range considered. The equations obtained from the linear fitting of the experimental data are as follows:

$$\begin{array}{cc} \text{CT AcP} & \text{M AcP} \\ C_m = 2.89 + 3.08\ \text{IS} & C_m = 4.00 + 3.69\ \text{IS} \end{array} \tag{3}$$

$$\Delta G(H_2O) = 17.2 + 18.3\ \text{IS} \quad \Delta G(H_2O) = 19.2 + 17.7\ \text{IS} \tag{4}$$

where C_m and ionic strength (IS) are expressed in units of molar and $\Delta G(H_2O)$ in units of kilojoules per mole. It can be seen that the dependence of C_m values on ionic strength is more pronounced for the muscle enzyme. However, the higher *m* value found for CT AcP under these experimental conditions relative to that of M AcP results in the dependence of $\Delta G(H_2O)$ on ionic strength being very similar for both isoenzymes.

Kinetics of Folding and Unfolding of CT AcP. The kinetics of folding of CT AcP were studied over a wide range of denaturant concentrations at 28 °C and pH 5.5. AcP was initially unfolded in 2 M urea (pH 1.9) or 7 M urea (pH 5.5). Refolding was then initiated by means of urea concentration and pH changes by rapid mixing, the final urea concentration ranging between 0 and 4 M and the final pH being 5.5. At very low urea concentrations, folding of CT AcP appears to be a biphasic process with a high-amplitude

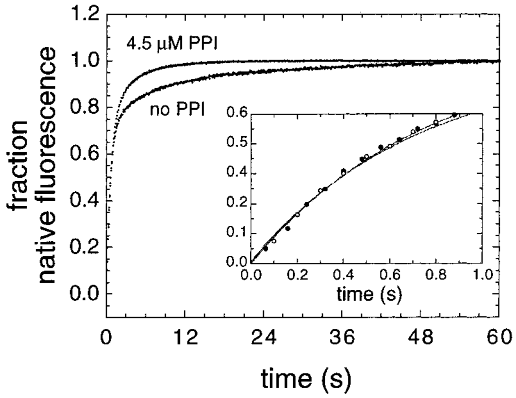

FIGURE 5: Folding of CT AcP in the presence and absence of 4.5 μM PPI. The final conditions are 50 mM acetate buffer at pH 5.5 and 28 °C. In the inset is depicted the folding in the presence (○) and absence (●) of 4.5 μM PPI monitored during the first second.

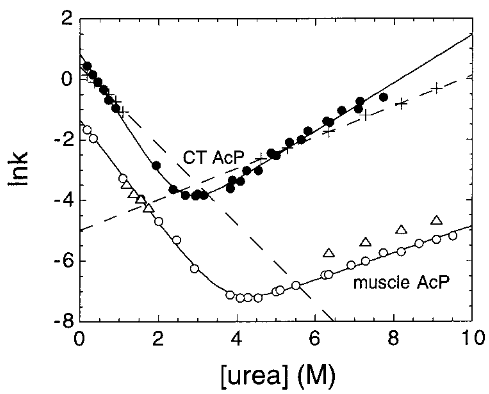

FIGURE 6: Natural logarithm of folding and unfolding rate constants of CT and M AcP as a function of urea concentration (28 °C): (●) CT AcP at pH 5.5, (○) M AcP at pH 5.5, (+) CT AcP at pH 9.2, and (△) M AcP at pH 9.2. The two sets of data at pH 5.5 were fitted to eq 1 (solid lines), while the folding and unfolding data of CT AcP at pH 9.2 were separately linearly fitted (dashed lines). M AcP is the Cys21Ser mutant.

fast phase strongly dependent on urea concentration, and a minor slow phase whose calculated rate constant (0.071 ± 0.010 s^{-1}) and relative amplitude (ca. 20%) are not affected by urea concentration. Such a slow phase was also observed for M AcP and was attributed to the proline isomerization rate-limited folding of a proportion of protein molecules (*16*). Figure 5 depicts the effect of peptidyl prolyl isomerase (PPI) on the folding kinetics of CT AcP at pH 5.5. While the fast phase is not affected by the addition of 4.5 μM PPI (Figure 5 inset), the rate of the slow phase is increased 3.5-fold under these conditions. The slow phase of CT AcP folding can therefore, like that for the muscle protein, be attributed to a proline isomerization rate-limited event.

The kinetics of unfolding of CT AcP were studied at pH 5.5 by diluting the native protein in the absence of urea into unfolding buffers containing various urea concentrations ranging from 4 to 8 M. The unfolding of CT AcP is a monophasic process under all conditions studied. In Figure 6, we summarize the natural logarithm of folding and unfolding rate constants as a function of urea concentration together with the data for M AcP as a comparison (*16*). The folding and unfolding data were globally fitted to eq 1, and the parameters determined by such an analysis are listed in Table 3. The thermodynamic parameters estimated from this kinetic study are in good agreement with those calculated

Table 3: Kinetic Analysis of Folding and Unfolding of CT and M AcP[a]

protein	k_{f,H_2O} (s^{-1})[b]	k_{u,H_2O} (s^{-1})[b]	m_f (M^{-1})[b]	m_u (M^{-1})[b]	C_m (M)[c]	m (kJ mol^{-1} M^{-1})[c]	ΔG (kJ mol^{-1})[c]	$\alpha^{\ddagger c}$
CT AcP (pH 5.5)	2.31	1.5×10^{-3}	2.04	0.80	2.6	7.1	18.3	0.28
M AcP[d] (pH 5.5)	0.23	1.1×10^{-4}	1.61	0.42	3.8	5.1	19.0	0.21
CT AcP (pH 9.2)	1.51	6.3×10^{-3}	1.33	0.52	3.0	4.6	13.7	0.28

[a] The experiments were performed in 50 mM acetate buffer (pH 5.5) or 50 mM tris/acetic acid buffer (pH 9.2) at 28 °C. Experimental errors are as follows: 8% for k_{f,H_2O} and k_{u,H_2O}, 5% for m_f and m_u, 0.3 M for C_m, 5% for m, 12% for ΔG, and 7% for $\alpha^{\ddagger}$. [b] Parameters obtained by fitting folding and unfolding rate constant data to eq 1. [c] Parameters obtained as described in Materials and Methods. [d] The enzyme is the Cys21Ser mutant, and the data are from ref *28*.

from equilibrium experiments under the same conditions, suggesting that a two-state model accounts for both the proteins under the studied conditions. Significant differences emerge, however, for the two isoenzymes with respect to the kinetic parameters. In particular, both folding and unfolding appear to be markedly faster for CT AcP. The folding and unfolding rate dependencies on urea concentration (i.e., m_f and m_u values) are also significantly higher than those of M AcP; this leads to a larger m value, as also observed in the equilibrium experiments. To address the differences between the m values observed for the two isoenzymes, we carried out a study at pH 9.2 where the m values of the two proteins are closer (Figure 3). Figure 6 shows that the refolding rate of M AcP is not significantly different at pH 9.2 and 5.5, whereas the unfolding is slightly accelerated; the m_f and m_u values are broadly unchanged at the two pH values. On the other hand, the plot of ln k versus urea concentration for CT AcP at pH 9.2 is notably different from that at pH 5.5. Although the rates of folding and unfolding are not significantly altered, the m_f and m_u values are markedly lower and comparable to those observed for M AcP (Table 3). This results in a global m value of 4.63 ± 0.30 kJ mol^{-1} M^{-1}, a value very similar to that calculated from equilibrium experiments at pH 9.2 (4.85 ± 0.35 kJ mol^{-1} M^{-1}). The m_f and m_u values reported in Table 3 allow the determination of the urea $\alpha^{\ddagger}$ value, a parameter related to the amount of surface area that is exposed to the solvent in the transition state for folding (*27*). The urea $\alpha^{\ddagger}$ value (0.28 ± 0.02) reported in Table 3 for CT AcP indicates that ca. 28% of the surface area exposed to the urea in the unfolded state is already exposed to the solvent in the transition state, at both pH 5.5 and 9.2 (*27*).

Folding Rate as a Function of Temperature. Figure 7 depicts the Eyring analysis of the folding rate of CT AcP at two different urea concentrations. The data for M AcP obtained previously (*28*) are also reported in the figure for comparison. The parameters determined by fitting to a model attributing the curvature of the plot solely to the heat capacity change (*22*) are summarized in Table 4, which also compares the activation thermodynamic parameters of CT AcP relative to those of the muscle enzyme (*28*). The heat capacity change upon moving from the folded state to the transition state on this model ($\Delta C_{pu}^{\ddagger}$) can be obtained as described previously (*28*). Dividing $\Delta C_{pu}^{\ddagger}$ by ΔC_p, as estimated by equilibrium experiments (Table 2), we obtained a value of fractional ΔC_p

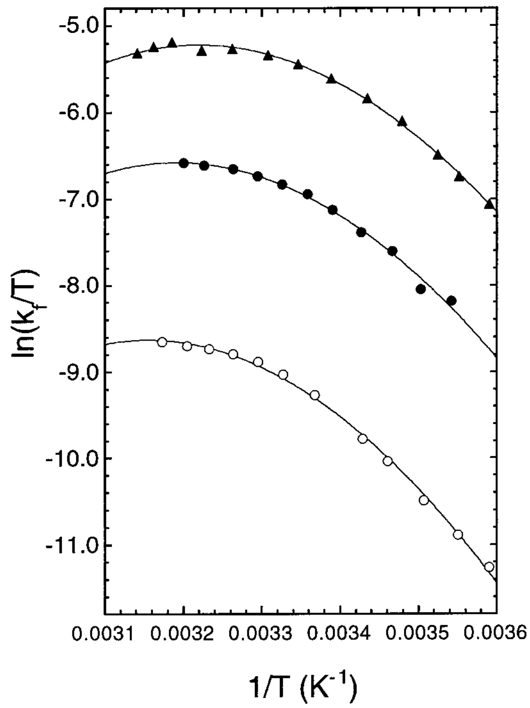

FIGURE 7: Eyring plot for folding of CT AcP at 0.18 M urea (▲), CT AcP at 1.1 M urea (●), and M AcP at 1.1 M urea (○). The data corresponding to M AcP are those reported previously (*28*). Under these conditions, folding of CT AcP consists of two phases where the slower phase can be attributed to proline isomerization. The data shown refer to the faster high-amplitude phase. The data were fitted as described by Chen et al. (*22*), and the parameters estimated by such a fitting procedure are summarized in Table 4.

which can be correlated with the fraction of hydrophobic moieties that become exposed to the solvent upon unfolding but which are solvent-accessible in the transition state (*22*). The fractional ΔC_p values for the two isoenzymes are given in Table 4 and are very similar. The enthalpy and entropy profiles show that the energetic barrier to folding at 28 °C results from both enthalpic and entropic contributions. For CT AcP, however, the entropic contribution is more pronounced than for M AcP.

DISCUSSION

The equilibrium unfolding curves of CT AcP determined by following the intrinsic fluorescence and CD signal are highly superimposable, indicating that all the structural changes associated with the denaturation of the protein occur through a highly cooperative transition. The ln k_f value is linearly related to urea concentration, and good agreement exists for all the thermodynamic parameters estimated from equilibrium and kinetic data, indicating that CT AcP folds according to a two-state model over the entire urea concentration range (0−8 M) examined in this study (*21*, *29*). The *m* value measured in equilibrium experiments is slightly lower than that calculated from the kinetic data (Tables 1 and 3). This discrepancy could be simply due to the uncertainties of the measurements. Nevertheless, we cannot rule out the possibility that this difference arises from the presence of native-like intermediates containing non-native cis Xaa−Pro peptide bonds that are significantly populated at equilibrium. This possibility would be supported by recent observations indicating that a small fraction of the molecules of AcP folds via a rearrangement of a native-like intermediate containing the Ser70−Pro71 peptide bond in a non-native cis conformation (F. Chiti and C. M. Dobson, unpublished results).

Temperature Dependence of the Unfolding Thermodynamics. A complete characterization of the thermodynamics of unfolding requires the determination of the free energy, enthalpy, and entropy changes occurring during the reaction. The ΔH and ΔS values that could be obtained with van't Hoff analysis applied to thermal denaturation are limited to the high temperatures at which thermal denaturation occurs (54 °C for CT AcP). Extrapolation to room temperature requires estimation of the ΔC_p value; this parameter is also needed for a complete study of the temperature dependence of $\Delta G(H_2O)$. Calorimetric techniques provide a means for determining the ΔC_p value, but thermally unfolded CT AcP tends to aggregate at the high concentrations needed for this technique. We therefore applied the procedure introduced by Agashe and Udgaonkar (*23*) and Scholtz (*30*), and obtained a ΔC_p value for CT AcP in close agreement with that of M AcP (*15*). As the ΔC_p value is correlated with the exposure of hydrophobic moieties upon denaturation (*31*) and the degree of sequence homology for the hydrophobic cores of the two proteins is very high (*10*), the finding that the two proteins have similar ΔC_p values is reasonable.

The ΔH and $T\Delta S$ values at 25 °C (114 ± 15 kJ mol^{-1} and 96 ± 12 kJ mol^{-1} K^{-1}, respectively) indicate that the native conformation of CT AcP is stabilized by a favorable enthalpic contribution which outweighs an unfavorable entropic one (all the values and their signs refer to the unfolding reaction), in agreement with results provided by calorimetry for other proteins (*32*).

Dependence of the m Value upon Temperature, Ionic Strength, and pH. The urea *m* value for CT AcP exhibits only a small temperature dependence, as found for other proteins (*23*, *24*, *30*). The ionic strength does not affect this parameter for AcP, suggesting that the degrees of surface area exposure of the folded and unfolded states do not change significantly with variations in either temperature or ionic strength. By contrast, the *m* value has a marked dependence on pH (Figure 3), in agreement with findings for M AcP (*15*) and other proteins (*33*, *34*). Low pH values lead to an increase in the *m* value to nearly twice that at neutral pH. This experimental observation has been attributed to the accumulation of positive charges on the surface of the protein at low pH values, resulting in an increase in the average dimensions of the unfolded conformation relative to the folded state (*33*). In this regard, however, it is important to note that for CT AcP a comparable increase in the *m* value at high pH values is not clearly observed. A possible explanation might be sought in the basic isoelectric point of CT AcP that means studies of urea denaturation cannot be extended to pH values where the enzyme carries an excess negative charge.

In both enzymes, the *m* value reaches a minimum at mildly basic pH, corresponding to a minimum in the net charge of the protein. Indeed, the theoretical isoelectric points of CT and M AcP are 9.3 and 9.6, respectively, as calculated by the software *ProtParam Tool* (http://www.expasy.ch/sprot/protparam.html). This observation is consistent with the importance of the net charge of the protein in determining the average dimensions of the unfolded state and consequently the magnitude of the *m* value. An interesting finding

Table 4: Activation Thermodynamic Parameters of CT and M AcP Folding[a]

protein	$\Delta G_f^{\ddagger}$ (kJ mol^{-1})	$\Delta H_f^{\ddagger}$ (kJ mol^{-1})	$T\Delta S_f^{\ddagger}$ (kJ mol^{-1})	$\Delta C_{pf}^{\ddagger}$ (kJ mol^{-1} K^{-1})	fractional ΔC_p
CT AcP (0.18 M urea)	72.9	23.6	−49.3	−2.48	0.60
CT AcP (1.1 M urea)	76.6	30.1	−46.1	−2.49	0.59
M AcP (1.1 M urea)	82.1	40.7	−41.4	−2.57	0.59

[a] All the activation parameters refer to the U → TS reaction at 28 °C. For CT AcP, the analysis was carried out by fitting the data shown in Figure 7 according to the methods of Chen et al. (*22*). The values of M AcP are those reported previously (*28*). Experimental errors are as follows: 0.5% for $\Delta G_f^{\ddagger}$, 10% for $\Delta H_f^{\ddagger}$ and $T\Delta S_f^{\ddagger}$, 5% for $\Delta C_{pf}^{\ddagger}$, and 10% for fractional ΔC_p.

is that the *m* value is reduced for CT AcP but not for M AcP upon increasing the pH from 8 to 9, a jump observed in both equilibrium and kinetic experiments. A possible explanation for this behavior could be found in the differences in the amino acid compositions of the two proteins (*10*). The content of titratable amino acids in the two enzymes differs basically for the presence, in human CT AcP, of three histidine residues which are typically absent in M AcP. Under conditions of mildly acid pH, such as the pH value of maximum conformational stability of both proteins, all of the histidine residues are likely to be charged in the unfolded state. An increase of pH above 8 will cause the complete deprotonation of these residues (*35*), reducing the positive net charge of CT AcP and eliminating the differences between the two enzymes as the pH approaches the isoelectric points. As a consequence, the *m* value would be reduced to the value of M AcP (Figure 3).

Effect of Ionic Strength on Protein Stability. The free energy of unfolding increases linearly with ionic strength, the magnitude of this increase being very similar for the two isoenzymes (Figure 4 and eq 4). An explanation for this is likely to be associated with the exclusion of ions from the surface area of the protein preferentially destabilizing the unfolded conformation. In addition, ionic compounds will alter the solvent dielectric constant with the ultimate effect of increasing the free energy of the unfolded state via a destabilization of the exposed hydrophobic groups. Two considerations, however, suggest that denaturation of CT and M AcP results in a similar degree of exposure of hydrophobic groups. First, the amino acid composition identity is very high for the two proteins at the level of the hydrophobic core (75%) and approaches 100%, if conservative substitutions are considered (*10*). Second, and more importantly, the experimentally determined ΔC_p values of the two proteins are very similar (Table 2). Therefore, the very similar increase in stability for the two proteins upon the addition of salts is likely to arise from a similar exposure of buried groups, particularly hydrophobic residues, following denaturation.

Thermodynamics of the Transition State for Folding. Application of the Eyring analysis to the temperature dependence of the folding rate constant allows the quantification of the thermodynamic parameters upon moving from the unfolded to the transition state. Interpretation of the $\Delta H_f^{\ddagger}$ and $\Delta S_f^{\ddagger}$ values to obtain structural details of the transition state is, however, difficult. The conformation and intramolecular contacts within the polypeptide chain are not the sole factors contributing to the magnitude of the two values, as an important role is played by the protein−water interactions. The fractional ΔC_p and the urea $\alpha^{\ddagger}$ value are more informative from this point of view and are more directly related to the fraction of surface area, exposed in the unfolded state and buried in the folded state, that is still solvent-accessible in the transition state (*27*, *36*−*38*). Such values were found to be significantly different (Table 3), a discrepancy observed for both isoenzymes and other proteins (*39*). This inconsistency may be attributed to the different nature of the sites interacting with the solvent probed with the two methods (*28*) or, alternatively, to nonspecific viscosity effects involved in the two measurements (K. W. Plaxco, personal communication).

An interesting feature arising from the kinetic analysis performed on CT AcP at pH 9.2 is the significant change of both the m_f and m_u parameters from the values found for the same isoenzyme at pH 5.5. In addition, both the parameters calculated for CT AcP at pH 9.2 are fairly similar to those found for M AcP at pH 5.5 (Table 3). The m_u and m_f values correlate with the solvent-accessibility changes of the protein surface area upon moving from the folded state to the transition state and from the transition state to the unfolded state, respectively (*21*, *27*). If it is assumed that the compactness of the folded state is not substantially changed at the different pH values, the experimental observation that both m_u and m_f values are lowered for CT AcP when the pH is increased from 5.5 to 9.2 could suggest that deprotonation of the histidine residues causes a reduction in the degree of solvent exposure of the surface area, not just for the unfolded state but also for the transition state, though for the latter to a lesser extent. Under these experimental conditions, CT AcP behaves in a manner similar to that of M AcP, which indeed lacks the histidine residues.

Comparison of the Folding Properties of CT and M AcP. The equilibrium analysis of CT AcP as a function of temperature, pH, and ionic strength has been carried out at 25 °C and compared with that of M AcP obtained previously under similar conditions (*15*). In contrast, a temperature of 28 °C has been chosen for the kinetic experiments so a comparison with the data of M AcP reported in previous works at the same temperature could be carried out (*16*, *28*). In these papers, the Cys21Ser mutant of M AcP has been used for the kinetic analysis due to problems arising from oxidation of a free cysteine residue (*16*). The folding and unfolding rates of the M AcP species carrying a reduced cysteine residue are, respectively, only 1.2 and 1.6 times lower than those of the C21S mutant. These similarities are not surprising given the superficial location of Cys21 and the lack of noncovalent interactions involving this residue and validate the use of the C21S mutant for the characterization of folding of M AcP and for its comparison with CT AcP.

Both CT and M AcP exhibit two-state folding behavior over the whole range of urea concentrations and fold rather slowly compared to most of two-state folding proteins (*39*, *40*). They feature a second low-amplitude slower phase that can be attributed to proline isomerization. Despite these similarities, a number of important differences between the two isoenzymes emerge. (i) CT AcP appears to be less stable under all conditions of temperature, pH, and ionic strength studied, regardless of whether we consider the unfolding ΔG or the midpoint of thermal or chemical denaturation as an index of protein stability. (ii) In the absence of denaturant at pH 5.5 and 25 °C, folding and unfolding of CT AcP are, respectively, some 10 and 14 times faster than those of M AcP. The folding rate of CT AcP is accelerated relative to that of M AcP to a lesser extent than the unfolding rate, hence explaining the lower free energy of CT AcP compared to that of M AcP. The fact that the least stable variant exhibits the highest folding rate indicates that there is not a simple relationship between conformational stability and folding rate for AcP, an observation supported by the comparison of the folding properties of other highly homologous proteins such as the SH3 domains isolated from a number of proteins (*41*). The difference in the folding and unfolding rates between the two isoenzymes is maintained throughout the range of conditions examined here and is therefore likely to be a result, to a first approximation, of a more stable folding transition state, relative to the folded and unfolded states, for CT AcP compared to M AcP. (iii) A significant difference in the *m* value has been observed. This difference is likely to arise from a larger number of sites exposed to the solvent and interacting with urea in the unfolded state of CT AcP relative to that in the muscle enzyme. Despite a more compact unfolded state, M AcP exhibits a slower folding rate. Moreover, the increase of the denatured state compactness found in CT AcP following the increase of pH does not lead to an acceleration of folding in this protein. The difference in *m* values found for the two proteins is not observed for the fractional ΔC_p value, a parameter also correlated with the solvent-exposed surface area change upon unfolding. As this parameter can be specifically correlated with the degree of exposure of hydrophobic residues upon unfolding (*31*), the possible presence of a further electrostatic repulsion in unfolded CT AcP, arising from the presence of three more charged histidines and inducing the expansion of the unfolded state, is likely to involve mainly polar groups which can interact with urea. Interestingly, the higher degree of solvent exposure of the unfolded state of CT AcP relative to that of M AcP and involving this kind of groups is not associated with a reduction of the folding rate.

ACKNOWLEDGMENT

We thank Sophie Jackson for providing PPI.

REFERENCES

1. Evans, P. A., and Radford, S. E. (1994) *Curr. Opin. Struct. Biol. 4*, 100−106.
2. Roder, H., and Elove, G. A. (1994) in *Mechanisms of protein folding* (Pain, R. H., Ed.) pp 26−54, IRL Press, Oxford, U.K.
3. Plaxco, K. W., and Dobson, C. M. (1996) *Curr. Opin. Struct. Biol. 6*, 630−636.
4. Kim, P. S., and Baldwin, R. L. (1990) *Annu. Rev. Biochem. 59*, 631−660.
5. Karplus, M., and Weaver, D. L. (1994) *Protein Sci. 3*, 650−668.
6. Fersht, A. R. (1997) *Curr. Opin. Struct. Biol. 7*, 3−9.
7. Shakhnovich, E. I. (1997) *Curr. Opin. Struct. Biol. 7*, 29−40.
8. Miranker, A., and Dobson, C. M. (1996) *Curr. Opin. Struct. Biol. 6*, 31−42.
9. Dobson, C. M., Sali, A., and Karplus, M. (1998) *Angew. Chem., Int. Ed. 37*, 868−893.
10. Stefani, M., Taddei, N., and Ramponi, G. (1997) *Cell. Mol. Life Sci. 53*, 141−151.
11. Nassi, P., Nediani, C., Liguri, G., Taddei, N., and Ramponi, G. (1991) *J. Biol. Chem. 266*, 10867−10871.
12. Nediani, C., Fiorillo, C., Marchetti, E., Pacini, A., Liguri, G., and Nassi, P. (1996) *J. Biol. Chem. 271*, 19066−19073.
13. Pastore, A., Saudek, V., Ramponi, G., and Williams, R. J. P. (1992) *J. Mol. Biol. 224*, 427−440.
14. Thunnissen, M. M. G. M., Taddei, N., Liguri, G., Ramponi, G., and Nordlund, P. (1997) *Structure 5*, 69−79.
15. Chiti, F., Van Nuland, N. A. J., Taddei, N., Magherini, F., Stefani, M., Ramponi, G., and Dobson, C. M. (1998) *Biochemistry 37*, 1447−1455.
16. van Nuland, N. A. J., Chiti, F., Taddei, N., Raugei, G., Ramponi, G., and Dobson, C. M. (1998) *J. Mol. Biol. 283*, 883−891.
17. Fiaschi, T., Raugei, G., Marzocchini, R., Chiarugi, P., Cirri, P., and Ramponi, G. (1995) *FEBS Lett. 367*, 145−148.
18. Laemmli, U. K. (1970) *Nature 227*, 680−685.
19. Chiti, F., Magherini, F., Taddei, N., Ilardi, C., Stefani, M., Bucciantini, M., Dobson, C. M., and Ramponi, G. (1998) *Protein Eng. 11*, 557−561.
20. van Nuland, N. A. J., Meijberg, W., Warner, J., Forge, V., Scheek, R. M., Robillard, G. T., and Dobson, C. M. (1998) *Biochemistry 37*, 622−637.
21. Jackson, S. E., and Fersht, A. R. (1991) *Biochemistry 30*, 10428−10435.
22. Chen, B. L., Baase, W. A., and Schellman, J. A. (1989) *Biochemistry 28*, 691−699.
23. Agashe, V. R., and Udgaonkar, J. B. (1995) *Biochemistry 28*, 3286−3299.
24. Nicholson, E. M., and Scholtz, J. M. (1996) *Biochemistry 35*, 11369−11378.
25. Linderstrom-Lang, K. (1924) *C. R. Trav. Lab. Carlsberg*, 15−70.
26. Liguri, G., Camici, G., Manao, G., Cappugi, G., Nassi, P., Modesti, A., and Ramponi, G. (1986) *Biochemistry 25*, 8089−8094.
27. Tanford, C. (1970) *Adv. Protein Chem. 24*, 1−95.
28. Chiti, F., Taddei, N., van Nuland, N. A. J., Magherini, F., Stefani, M., Ramponi, G., and Dobson, C. M. (1998) *J. Mol. Biol. 283*, 893−903.
29. Matouschek, A., Kellis, J. T., Serrano, L., and Fersht, A. R. (1989) *Nature 340*, 122−126.
30. Scholtz, J. M. (1995) *Protein Sci. 4*, 35−43.
31. Murphy, K. P., and Freire, E. (1992) *Adv. Protein Chem. 43*, 313−361.
32. Makhatadze, G. I., and Privalov, P. L. (1992) *J. Mol. Biol. 226*, 491−505.
33. Pace, C. N., Laurents, D. V., and Erickson, R. E. (1992) *Biochemistry 31*, 2728−2734.
34. Pace, C. N., and Vanderburg, K. E. (1979) *Biochemistry 18*, 288−292.
35. Creighton, T. E. (1993) *Proteins*, p 6, Freeman and Co., New York.
36. Spolar, R. S., Livingstone, J. R., and Record, M. T. (1992) *Biochemistry 31*, 3947−3955.
37. Jackson, S. E., and Fersht, A. R. (1991) *Biochemistry 30*, 10436−10443.
38. Livingstone, J. R., Spolar, R. S., and Record, M. T. (1991) *Biochemistry 30*, 4237−4244.
39. Plaxco, K. W., Simons, K. T., and Baker, D. (1998) *J. Mol. Biol. 277*, 985−994.
40. Viguera, A. R., Villegas, V., Aviles, F. X., and Serrano, L. (1996) *Folding Des. 2*, 23−33.
41. Plaxco, K. W., Guijarro, J. I., Morton, C. J., Pitkeathly, M., Campbell, I. D., and Dobson, C. M. (1998) *Biochemistry 37*, 2529−2537.

BI9822630